HHS Public Access

Author manuscript

Dev Dyn. Author manuscript; available in PMC 2023 December 09.

Published in final edited form as:

Dev Dyn. 2023 June ; 252(6): 761–769. doi:10.1002/dvdy.578.

Lack of evidence that fibrillin1 regulates bone morphogenetic protein 4 activity in kidney or lung

Autumn McKnite[#],

Hyung-Seok Kim[#],

Joshua Silva,

Jan L. Christian

Departments of Neurobiology and Internal Medicine, Division of Hematology and Hematologic Malignancies, University of Utah, School of Medicine, Salt Lake City, Utah, USA

[#] These authors contributed equally to this work.

Abstract

Background: The Bone morphogenetic protein 4 (BMP4) precursor protein is cleaved at two sites to generate an active ligand and inactive prodomain. The ligand and prodomain form a noncovalent complex following the first cleavage, but dissociate after the second cleavage. Transient formation of this complex is essential to generate a stable ligand. Fibrillins (FBNs) bind to the prodomains of BMPs, and can regulate the activity of some ligands. Whether FBNs regulate BMP4 activity is unknown.

Results: Mice heterozygous for a null allele of *Bmp4* showed incompletely penetrant kidney defects and females showed increased mortality between postnatal day 6 and 8. Removal of one copy of *Fbn1* did not rescue or enhance kidney defects or lethality. The lungs of $Fbn1^{+/-}$ females had enlarged airspaces that were unchanged in $Bmp4^{+/-}$;$Fbn1^{+/-}$ mice. Additionally, removal of one or both alleles of *Fbn1* had no effect on steady state levels of BMP4 ligand or on BMP activity in postnatal lungs.

Conclusions: These findings do not support the hypothesis that FBN1 plays a role in promoting BMP4 ligand stability or signaling, nor do they support the alternative hypothesis that FBN1 sequesters BMP4 in a latent form, as is the case for other BMP family members.

Correspondence Jan L. Christian, Department of Neurobiology, University of Utah, 20 South 2030 East, Bldg 570 BPRB, Rm 320, Salt Lake City, UT 84112, USA. jan.christian@neuro.utah.edu.

AUTHOR CONTRIBUTIONS

Autumn McKnite: Conceptualization (equal); formal analysis (equal); investigation (supporting); methodology (supporting); writing – original draft (supporting); writing – review and editing (supporting). **Hyung-Seok Kim:** Data curation (supporting); formal analysis (equal); validation (supporting); writing – review and editing (supporting). **Joshua Silva:** Formal analysis (supporting); methodology (supporting); writing – review and editing (supporting). **Jan L. Christian:** Conceptualization (lead); funding acquisition (lead); investigation (lead); methodology (equal); project administration (lead); supervision (lead); writing – original draft (lead); writing – review and editing (lead).

ETHICS STATEMENT

All experiments were conducted in accordance with local ethics regulations (University of Utah).

CONFLICT OF INTEREST STATEMENT

None disclosed.

Keywords

BMP4; fibrillin1; kidney; lung; mouse

1 | INTRODUCTION

Bone Morphogenetic Protein 4 (BMP4) is a member of the Transforming growth factor ß (TGFß) family of cell signaling molecules, which are required for proper embryonic development and adult homeostasis. In mice, null mutations in *Bmp4* lead to early embryonic lethality[1] while tissue-specific or hypomorphic mutations cause a broad spectrum of defects in multiple organs including the eye, skeleton, brain, heart, lungs and urogenital Autumn McKnite and Hyung-Seok Kim contributed equally to this work. systems.[2] Conversely, mutations that lead to a gain of BMP function cause embryonic lethality in animal models,[3] and ectopic bone formation in humans.[3,4] Thus, BMP activity must be strictly regulated to prevent congenital anomalies.

BMP4, like all TGFß proteins, is made as an inactive precursor protein that dimerizes and is cleaved by members of the proprotein convertase (PC) family to generate the active, disulfide-bonded ligand dimer and two prodomain monomers (illustrated in Figure 1A).[5] Although the prodomain lacks signaling activity, it is essential for generation of an active ligand. Proteolytic activation of BMP4 is unique in that it occurs sequentially at two sites:initially at a PC motif (R-X-K-R) adjacent to the ligand domain (the S1 site) and subsequently at an upstream R-X-X-R motif (the S2 site) within the prodomain.[6,7] Following the first cleavage, the BMP4 ligand forms a transient, non-covalent complex with the prodomain but subsequent cleavage at the S2 site disrupts the complex, freeing the ligand (Figure 1A).[8]

Cleavage of both sites of BMP4, and formation of the transient prodomain/ligand complex is essential to generate a stable, fully active ligand.[9,10] Mice carrying a knockin point mutation (*Bmp4*^{S2K}) that causes simultaneous rather than sequential cleavage of both prodomain sites show loss of BMP4 function and die during mid-embryogenesis.[10] Levels of cleaved BMP4 ligand are severely reduced in mutants, although levels of precursor and cleaved prodomain are unchanged relative to wild type. These findings demonstrate that formation of the transient BMP4 prodomain/ligand complex is essential to stabilize the ligand after its release from the prodomain, but how it does so is unknown.

Proteolytic cleavage of BMP4 occurs in a post-TGN compartment, coincident with secretion from the cell,[10] raising the possibility that the prodomain interacts with extracellular matrix (ECM) proteins to target the ligand to binding partners that protect it from degradation. Fibrillin1 and fibrillin2 (FBNs) are major components of ECM microfibrils that bind either directly or indirectly to the prodomains of TGFß1–3, BMP2, 4, 7, 10, and growth and differentiation factor5 (GDF5).[11] This has been proposed to either sequester the ligand in the matrix in an inactive form or to facilitate signaling.[12] For example, the prodomain of TGFß1 binds to the cleaved ligand, and to adaptor proteins called latent TGFß binding proteins (LTBPs) that in turn associate with FBNs. FBNs sequester the ligand/prodomain/LTBP complex in the ECM in a latent, inactive form.[13] By contrast, the BMP7 ligand forms

a stable noncovalent complex with its prodomain following cleavage[14,15] but can still bind and activate BMP receptors in solution.[16] When the prodomain binds to FBNs, however, a conformational shift occurs that prevents the ligand from activating receptors.[17] Consistent with this biochemical model in which FBNs sequester BMP7 in an inactive form, *Fbn2* null mutant mice display elevated BMP signaling activity and develop myopathy that is partially rescued by deletion of one allele of *Bmp7*.[18] Furthermore, a failure to downregulate FBN2 in the developing skeleton leads to impaired BMP signaling, at least in part due to sequestration of latent GDF5.[19] Analysis of total BMP activity in osteoblasts isolated from *Fbn1* mutant mice, or derived from humans carrying mutations in *FBN1*, suggests that FBN1 may either sequester BMP ligands in the matrix in an inactive form,[20] or may enhance BMP activity.[21] Collectively, these findings suggest that FBNs interact with, and regulate the activity of different BMP family members in a ligand-and tissue-specific fashion.

Unlike TGFß, BMP7 or GDF5, the BMP4 ligand is released from the prodomain following cleavage, making it unlikely that FBNs sequester the ligand in the matrix. We have previously hypothesized that FBNs anchor the transient BMP4 prodomain/ligand complex in the ECM following S1 cleavage, and that this enables the ligand to be passed off to other ECM components that protect it from degradation following S2 cleavage (illustrated in Figure 1B).[10] Specifically, we suggest that FBN binds to the prodomain portion of the BMP4 precursor protein within the secretory pathway, prior to cleavage. When the S1 site is cleaved, this generates a FBN bound prodomain/ligand complex (Figure 1B). This transient complex serves to deposit mature BMP4 in the ECM coincident with S2 cleavage, thereby facilitating association with heparin sulfate proteoglycans (HSPGs), collagens or other binding proteins that are critical for ligand stability and/or signaling. This model offers an explanation for the severe loss of function observed in $Bmp4^{S2K}$ mutant mice, because in these mice both sites are cleaved simultaneously, which would prevent formation of the transient fibrillin/prodomain/mature domain complex (Figure 1C). In this case, mature BMP4 would be released from the fibrillin bound prodomain prematurely, precluding efficient association with HSPGs or other ECM proteins that are required to stabilize the free ligand (Figure 1C). This would account for the specific reduction in levels of cleaved ligand but not cleaved prodomain in $Bmp4^{S2KHAmyc}$ mutant mice,[10] since the prodomain remains anchored in the ECM regardless of the order of cleavages. In the current studies we use genetic and biochemical analyses to begin to test whether FBN1 is required to enhance or inhibit the activity of BMP4.

2 | RESULTS AND DISCUSSION

2.1 | Removal of one copy of *Fbn1* does not enhance lethality of $Bmp4^{+/-}$ mice

To look for genetic interactions between *Fbn1* and *Bmp4*, we crossed mice heterozygous for a null allele of *Fbn1* ($Fbn1^{+/-}$) with mice heterozygous for a null allele of *Bmp4* ($Bmp4^{+/-}$) and assessed survival at weaning. If interactions between FBN1 and the BMP4 prodomain/ligand complex are essential for full BMP4 activity, then reducing *Fbn1* gene dosage will lead to a further reduction in BMP4 signaling in $Bmp4^{+/-}$ mice, due to destabilization of the ligand. $Bmp4^{+/-}$ and $Bmp4^{+/-};Fbn1^{+/-}$ mice were underrepresented at weaning (Table 1A) consistent with previous findings showing that a single copy of *Bmp4* is not

sufficient to support full viability.[22] *Bmp4*$^{+/-}$ and *Bmp4*$^{+/-}$;*Fbn1*$^{+/-}$ female mice, but not males, were significantly underrepresented at postnatal day (P)21 (Table 1A) and at P8 (Table 1B), but not at P6 (Table 1C). There was no significant difference in survival of *Bmp4*$^{+/-}$;*Fbn1*$^{+/-}$ mice relative to *Bmp4*$^{+/-}$ mice in either sex at any age. Thus, a subset of females heterozygous for a null allele of *Bmp4* die perinatally between P6 and P8, and additional removal of one copy of *Fbn1* neither rescues nor enhances the frequency or age of death.

2.2 | Removal of one allele of *Fbn1* does not alter the penetrance of kidney defects in *Bmp4*$^{+/-}$ mice

BMP4 function is required to inhibit ectopic budding from the ureter stalk, and to promote the elongation of the branching ureter to promote normal kidney morphogenesis.[23] In mice heterozygous for a null allele of *Bmp4*, disruption of these critical functions leads to abnormalities in kidney development including hydronephrosis, cystic kidneys, hydroureter and bifid ureter that mimic human congenital anomalies of the kidney and urinary tract.[23] We asked whether removal of one allele of *Fbn1* in *Bmp4*$^{+/-}$ mice exacerbates or moderates these defects. Kidney defects were never observed in wildtype (Figure 2A) (n = 9) or *Fbn1*$^{+/-}$ (n = 13) mice. By contrast, consistent with published studies,[22,23] 50% of *Bmp4*$^{+/-}$ pups (n = 12) displayed hydronephrosis, hydroureter, bifid ureter, and/or hypoplastic or polycystic kidneys at P5 (Figure 2B-D). There was no difference in gross morphology (Figure 2E-G) or in the penetrance of these defects in *Bmp4*$^{+/-}$;*Fbn1*$^{+/-}$ mice (44%, n = 9).

2.3 | FBN1 and BMP4 are co-expressed in airway epithelial cells of the developing lung

Bmp4 and *Fbn1* are co-expressed in some regions of the developing lung, and both have been reported to be required for normal lung development,[24,25] raising the possibility that they may functionally interact in this organ. *Bmp4* is strongly expressed in airway epithelial cells and in the adjacent mesenchyme from embryonic (E) day 11 and continues to be expressed in the lung after birth.[26] We co-immunostained sections of E15.5 lungs with antibodies specific for PECAM1, which marks vascular endothelial cells, and for FBN1. Consistent with previous studies,[27] FBN1 was expressed in airway epithelial cells (Figure 3A,C, yellow arrows) as well as in endothelial cells of arterioles and venules (white arrows). We also co-immunostained sections of lungs from *Bmp4*$^{+/-}$ mice (in which exon 3 is replaced with nuclear lacZ to generate a null allele[28]) with antibodies specific for FBN1 and ß-galactosidase, which marks cells expressing *Bmp4*. ß-galactosidase was detected in the nuclei of cells that co-express FBN1 (Figure 3D-F, blue arrowheads) and in cells adjacent to the FBN1 expressing cells (white arrowheads). Single cell sequencing confirms that *Fbn1* and *Bmp4* are both expressed in mesenchymal progenitors, myofibroblasts/smooth muscle, matrix fibroblasts as well as in epithelial cells of the developing lung.[29] Although *Fbn2* is co-expressed with *Fbn1* in many developing tissues including the lung, it is downregulated by mid- to late-gestation.[27]

2.4 | *Fbn1*$^{+/-}$ and *Bmp4*$^{+/-}$;*Fbn1*$^{+/-}$ females have enlarged airspaces in the lungs

Removal of one or both copies of *Fbn1*, or conditional deletion of one copy of *Bmp4* from airway epithelial cells leads to enlarged air spaces and abnormal lung morphogenesis.[24,25] Based on the similar lung phenotype in mice lacking one copy of *Bmp4* or *Fbn1*, we

wanted to know whether we could detect a genetic interaction between *Bmp4* and *Fbn1* in the lung. *Fbn1*$^{+/-}$ and *Bmp4*$^{+/-}$ mutants were intercrossed and litters collected at P5 to ask whether lung defects were exacerbated in compound heterozygotes. Histological analysis of lungs did not reveal gross differences in cell shape or morphology (Figure 4A). Surprisingly, no differences were observed in airspace size in *Bmp4*$^{+/-}$ mutants relative to wild type littermates, as quantified by mean linear intercept (MLI) lung morphometry (Figure 4B). As previously reported,[25] airspace size was enlarged in *Fbn1*$^{+/-}$ mice relative to wild type littermates (Figure 4B). Although airspace size trended slightly lower in *Bmp4*$^{-/-}$;*Fbn1*$^{+/-}$ mice, the enlarged airspace size was not significantly rescued nor exacerbated in *Bmp4*$^{-/-}$;*Fbn1*$^{+/-}$ mice relative to *Fbn1*$^{+/-}$ mutants (Figure 4B). When mice were stratified by sex, enlarged airspaces were observed in the lungs of female, but not male *Fbn1*$^{+/-}$ and *Bmp4*$^{-/-}$;*Fbn1*$^{+/-}$mice relative to controls (Figure 4C,D). Enlarged airspaces in the lungs of mice heterozyogous or homozygous for a null allele of *Fbn1* have been attributed to dysregulation of TGFß activation and signaling, resulting in apoptosis in the developing lung.[25] In these previous studies, mice were not stratified by sex, and it is not clear why this phenotype is observed only in females.

2.5 | Removal of one or both alleles of *Fbn1* does not alter BMP4 protein levels or total BMP activity in P5 lungs

To directly test whether FBN1 is required to stabilize mature BMP4 protein, we intercrossed *Fbn1*$^{+/-}$ mice and analyzed steady state levels of mature BMP4 protein in lungs isolated from littermates at P5, when FBN2 is no longer expressed.[27] Although there was some variability between levels of BMP4 ligand in mice of different genotypes even within the same litter, there was no significant difference in steady state levels of cleaved BMP4 ligand in mice that were wild type, heterozygous or homozygous for a null allele of *Fbn1* (Figure 5A-B,D,F). We also analyzed levels of phosphoSMAD1 (pSMAD1), which provides a direct readout of total BMP activity, in P5 lung samples from this same cohort of mice. There was no difference in pSmad1 levels in lungs isolated from *Fbn1*$^{+/+}$, *Fbn1*$^{+/-}$, *or Fbn1*$^{-/-}$ mice when all mice were analyzed together, or when stratified by sex (Figure 5A,C,E,G).

The current studies were an initial attempt to test the hypothesis that interactions between FBN1 and the BMP4 prodomain are essential for ligand stability or signaling. We did not find any phenotypic or biochemical evidence to support this hypothesis, or to support the alternative hypothesis that binding of FBN1 to the prodomain of BMP4 promotes latency, as is the case for BMP7 and GDF5.[18,19] BMP7 and GDF5 ligands both remain non-covalently associated with their respective prodomains following cleavage, which might explain why binding of FBNs to the BMP7 and GDF5 prodomain can promote ligand latency. By contrast, the BMP4 ligand is fully released from its prodomain, making it less likely that FBNs, which do not bind the ligand domain, can negatively regulate ligand activity following cleavage. A major limitation of this study is that FBN2 is co-expressed with FBN1 in many organs during development and may function redundantly with FBN1 to regulate BMP4 latency or stability. Another limitation is that our analysis was limited to viability, lung and kidney development whereas FBN1 or FBN2 may interact with BMP4 in an organ, or at a development stage that we did not analyze. Further studies, which are beyond the scope of the current analysis, will be needed to study these possibilities.

3 | EXPERIMENTAL PROCEDURES

3.1 | Mouse strains

Animal procedures followed protocols approved by the University of Utah Institutional Animal Care and Use Committees. *Bmp4*$^{+/-}$ and *Fbn1*$^{+/-}$ mice were obtained from Dr. B Hogan (Duke University) and Dr. F. Ramirez (Icahn School of Medicine at Mount Sinai), respectively. All mice are on a C57BL/6 background.

3.2 | Lung histology and MLI measurements

P5 lungs were flushed with ice cold 1×PBS delivered via the pulmonary vein until lungs appeared white (approximately 10 mL). A total of 5 mL of ice cold 4% paraformaldehyde in PBS was perfused through the lung via the trachea. Fixed lungs were dehydrated, embedded in paraffin, 10 μm sections cut and stained with Hematoxylin and eosin. MLI was calculated from a total of 8 to 10 images per sample as described.[30] All analysis was done in the green channel and a low-pass filter was applied to remove artifacts. Images were thresholded using Otsu's method[31] with a 16 pixel grid overlaid. Areas outside the lung image were excluded from measurement. Intercepts were identified as every threshold change along each individual line of the grid. For each image the mean linear intercept was given as the total length of lines within the lung image divided by the total number of intercepts.

3.3 | Immunohistochemistry

The thoracic cavity was dissected from embryos, fixed in 4% paraformaldehyde in PBS at 4° for 6 to 8 hours, incubated overnight in 30% sucrose in PBS at 4°C and then embedded in OCT (Tissue-Tek). A total of 10 μm cryosections were incubated overnight at 4°C with antibodies directed against FBN1 (1:500; rabbit p9543[32]), PECAM (1:500, BD Pharmingen 553 369) and/or ß-galactosidase (1:500, AbCam 9361–250) in PBS with 5% goat serum and 0.1% Triton X-100. Staining was visualized using Alexa Fluor 488- or 568-conjugated secondary antibodies (1:500; Molecular Probes).

3.4 | Immunoblot analysis

Lungs were dissected from pups at P5, homogenized in 1 mL 150 mM NaCl, 1% NP-40, 50 mM Tris pH 8.0 + complete Mini protease inhibitors (Roche), incubated on ice for 1 hour and spun down at 13000×*g* for 15 minutes at 4°C. Protein concentration was measured using a BCA kit (Thermo Scientific). Proteins were resolved by SDS-PAGE and transferred onto a PVDF membrane. Membranes were probed with anti-BMP4 (Santa Cruz, sc-12 721, 1:1000), anti pSMAD1 (Cell Signaling, 9511 S, 1:1000) or anti-ß Actin (AbCam, ab8227, 1:10 000) primary antibodies followed by HRP-conjugated anti-rabbit IgG or HRP-conjugated anti-mouse IgG2b heavy chain specific (Jackson ImmunoResearch) secondary antibodies. Immunoreactive proteins were visualized using an ECL prime kit (GE HealthCare).

3.5 | Statistical analysis

NIH image J software was used to quantify band intensity on immunoblots. All results were quantitated from a minimum of three biological replicates and variation was determined

using GraphPad Prism9 software to perform a Student's *t*-test to look for differences between paired samples (BMP4 protein levels in wild type versus *Fbn1* heterozygous or homozygous mutants, or differences in MLI between $Fbn1^{+/-}$ and $Fbn1^{+/-};Bmp4^{+/-}$ mice) and a Kruskal-Wallis test to compare MLI between three or more groups. $P < .05$ was considered significant.

ACKNOWLEDGMENTS

We thank Lynn Sakai (Oregon Health & Science University) for providing the FBN1 antibody and Mary Sanchez for managing the mouse colony, collecting and photographing kidneys. This work utilized DNA, peptide and imaging shared resources supported by the Huntsman Cancer foundation and the National Cancer Institute of the NIH (P30CA042014). The content is solely the responsibility of the authors and does not represent the official views of the NIH.

FUNDING INFORMATION

This work was supported by American Heart Association 15GRNT21800007 (Jan L. Christian), National Institutes of Health R01HD067473 and R01HD102668 (Jan L. Christian), University of Utah Funding Incentive Seed Grant (Jan L. Christian), and National Institutes of Health Developmental Biology Training Grant 5T32 HD07491 (Autumn McKnite).

Funding information

American Heart Association, Grant/Award Number: 15GRNT21800007; Eunice Kennedy Shriver National Institute of Child Health and Human Development, Grant/Award Numbers: 5T32 HD07491, R01HD067473, RO1HD102668; National Institute of Diabetes and Digestive and Kidney Diseases, Grant/Award Number: R01DK128068; University of Utah Funding Incentive Seed Grant, Grant/Award Number: 2019; National Cancer Institute of the NIH, Grant/Award Number: P30CA042014

DATA AVAILABILITY STATEMENT

All data are included in figures.

REFERENCES

1. Winnier G, Blessing M, Labosky PA, Hogan BL. Bone morphogenetic protein-4 is required for mesoderm formation and patterning in the mouse. Genes DevD. 1995;9(17):2105–2116.
2. Zhao GQ. Consequences of knocking out BMP signaling in the mouse. Genesis. 2003;35(1):43–56. doi:10.1002/gene.10167 [PubMed: 12481298]
3. Walsh DW, Godson C, Brazil DP, Martin F. Extracellular BMP-antagonist regulation in development and disease: tied up in knots. Trends Cell Biol. 2010;20(5):244–256. doi:10.1016/j.tcb.2010.01.008 [PubMed: 20188563]
4. Towler OW, Shore EM. BMP signaling and skeletal development in fibrodysplasia ossificans progressiva (FOP). Dev Dyn. 2022;251(1):164–177. doi:10.1002/dvdy.387 [PubMed: 34133058]
5. Bragdon B, Moseychuk O, Saldanha S, King D, Julian J, Nohe A. Bone morphogenetic proteins: a critical review. Cell Signal. 2011;23(4):609–620. doi:10.1016/j.cellsig.2010.10.003 [PubMed: 20959140]
6. Cui Y, Hackenmiller R, Berg L, et al. The activity and signaling range of mature BMP-4 is regulated by sequential cleavage at two sites within the prodomain of the precursor. Genes Dev. 2001;15(21):2797–2802. doi:10.1101/gad.940001 [PubMed: 11691831]
7. Cui Y, Jean F, Thomas G, Christian JL. BMP-4 is proteolytically activated by furin and/or PC6 during vertebrate embryonic development. EMBO J. 1998;17(16):4735–4743. doi:10.1093/emboj/17.16.4735 [PubMed: 9707432]
8. Degnin C, Jean F, Thomas G, Christian JL. Cleavages within the prodomain direct intracellular trafficking and degradation of mature bone morphogenetic protein-4. Mol Biol Cell. 2004;15(11):5012–5020. doi:10.1091/mbc.E04-08-0673 [PubMed: 15356272]

9. Goldman DC, Hackenmiller R, Nakayama T, et al. Mutation of an upstream cleavage site in the BMP4 prodomain leads to tissue-specific loss of activity. Development. 2006;133(10):1933–1942. doi:10.1242/dev.02368 [PubMed: 16624858]
10. Tilak A, Nelsen SM, Kim HS, et al. Simultaneous rather than ordered cleavage of two sites within the BMP4 prodomain leads to loss of ligand in mice. Development. 2014;141:3062–3071. doi: 10.1242/dev.110130 [PubMed: 24993941]
11. Sengle G, Charbonneau NL, Ono RN, et al. Targeting of bone morphogenetic protein growth factor complexes to fibrillin. J Biol Chem. 2008;283(20):13874–13888. doi:10.1074/jbc.M707820200 [PubMed: 18339631]
12. Zimmermann LA, Correns A, Furlan AG, Spanou CES, Sengle G. Controlling BMP growth factor bioavailability: the extracellular matrix as multi skilled platform. Cell Signal. 2021; 85:110071. doi:10.1016/j.cellsig.2021.110071
13. Rifkin D, Sachan N, Singh K, Sauber E, Tellides G, Ramirez F. The role of LTBPs in TGF beta signaling. Dev Dyn. 2022;251(1): 95–104. doi:10.1002/dvdy.331 [PubMed: 33742701]
14. Jones WK, Richmond EA, White K, et al. Osteogenic protein-1 (OP-1) expression and processing in Chinese hamster ovary cells: isolation of a soluble complex containing the mature and pro-domains of OP-1. Growth Factors. 1994;11(3):215–225. doi: 10.3109/08977199409046919 [PubMed: 7734147]
15. Gregory KE, Ono RN, Charbonneau NL, et al. The prodomain of BMP-7 targets the BMP-7 complex to the extracellular matrix. J Biol Chem. 2005;280(30):27970–27980. doi:10.1074/jbc.M504270200 [PubMed: 15929982]
16. Sengle G, Ono RN, Lyons KM, Bachinger HP, Sakai LY. A new model for growth factor activation: type II receptors compete with the prodomain for BMP-7. J Mol Biol. 2008;381(4):1025–1039. doi:10.1016/j.jmb.2008.06.074 [PubMed: 18621057]
17. Wohl AP, Troilo H, Collins RF, Baldock C, Sengle G. Extracellular regulation of bone morphogenetic protein activity by the microfibril component Fibrillin-1. J Biol Chem. 2016;291(24): 12732–12746. doi:10.1074/jbc.M115.704734 [PubMed: 27059954]
18. Sengle G, Carlberg V, Tufa SF, et al. Abnormal activation of BMP signaling causes myopathy in Fbn2 null mice. PLoS Genet. 2015;11(6):e1005340. doi:10.1371/journal.pgen.1005340
19. Mead TJ, Martin DR, Wang LW, et al. Proteolysis of fibrillin-2 microfibrils is essential for normal skeletal development. Elife. 2022;11:e71142. doi:10.7554/eLife.71142
20. Nistala H, Lee-Arteaga S, Smaldone S, et al. Fibrillin-1 and −2 differentially modulate endogenous TGF-beta and BMP bioavailability during bone formation. J Cell Biol. 2010;190(6): 1107–1121. doi:10.1083/jcb.201003089 [PubMed: 20855508]
21. Quarto N, Li S, Renda A, Longaker MT. Exogenous activation of BMP-2 signaling overcomes TGFbeta-mediated inhibition of osteogenesis in Marfan embryonic stem cells and Marfan patient-specific induced pluripotent stem cells. Stem Cells. 2012;30(12):2709–2719. doi:10.1002/stem.1250 [PubMed: 23037987]
22. Dunn NR, Winnier GE, Hargett LK, Schrick JJ, Fogo AB, Hogan BL. Haploinsufficient phenotypes in Bmp4 heterozygous null mice and modification by mutations in Gli3 and Alx4. Dev Biol. 1997;188(2):235–247. doi:10.1006/dbio.1997.8664 [PubMed: 9268572]
23. Miyazaki Y, Oshima K, Fogo A, Hogan BL, Ichikawa I. Bone morphogenetic protein 4 regulates the budding site and elongation of the mouse ureter. J Clin Invest. 2000;105(7):863–873. doi: 10.1172/JCI8256 [PubMed: 10749566]
24. Eblaghie MC, Reedy M, Oliver T, Mishina Y, Hogan BL. Evidence that autocrine signaling through Bmpr1a regulates the proliferation, survival and morphogenetic behavior of distal lung epithelial cells. Dev Biol. 2006;291(1):67–82. doi:10.1016/j.ydbio.2005.12.006 [PubMed: 16414041]
25. Neptune ER, Frischmeyer PA, Arking DE, et al. Dysregulation of TGF-beta activation contributes to pathogenesis in Marfan syndrome. Nat Genet. 2003;33(3):407–411. doi:10.1038/ng1116 [PubMed: 12598898]
26. Bellusci S, Henderson R, Winnier G, Oikawa T, Hogan BL. Evidence from normal expression and targeted misexpression that bone morphogenetic protein (Bmp-4) plays a role

in mouse embryonic lung morphogenesis. Development. 1996;122(6): 1693–1702. doi:10.1242/dev.122.6.1693 [PubMed: 8674409]

27. Zhang H, Hu W, Ramirez F. Developmental expression of fibrillin genes suggests heterogeneity of extracellular microfibrils. J Cell Biol. 1995;129(4):1165–1176. doi:10.1083/jcb.129.4.1165 [PubMed: 7744963]
28. Lawson KA, Dunn NR, Roelen BA, et al. Bmp4 is required for the generation of primordial germ cells in the mouse embryo. Genes Dev. 1999;13(4):424–436. doi:10.1101/gad.13.4.424 [PubMed: 10049358]
29. Du Y, Ouyang W, Kitzmiller JA, et al. Lung gene expression analysis web portal version 3: lung-at-a-glance. Am J Respir Cell Mol Biol. 2021;64(1):146–149. doi:10.1165/rcmb.2020-0308LE [PubMed: 33385216]
30. Knudsen L, Weibel ER, Gundersen HJ, Weinstein FV, Ochs M. Assessment of air space size characteristics by intercept (chord) measurement: an accurate and efficient stereological approach. J Appl Physiol (1985). 2010;108(2):412–421. doi:10.1152/japplphysiol.01100.2009 [PubMed: 19959763]
31. Otsu N. A threshold selection method from gray level histograms. IEEE Trans Syst. 1979;SMC-9:62–66.
32. Gayraud B, Keene DR, Sakai LY, Ramirez F. New insights into the assembly of extracellular microfibrils from the analysis of the fibrillin 1 mutation in the tight skin mouse. J Cell Biol. 2000;150(3):667–680. doi:10.1083/jcb.150.3.667 [PubMed: 10931876]

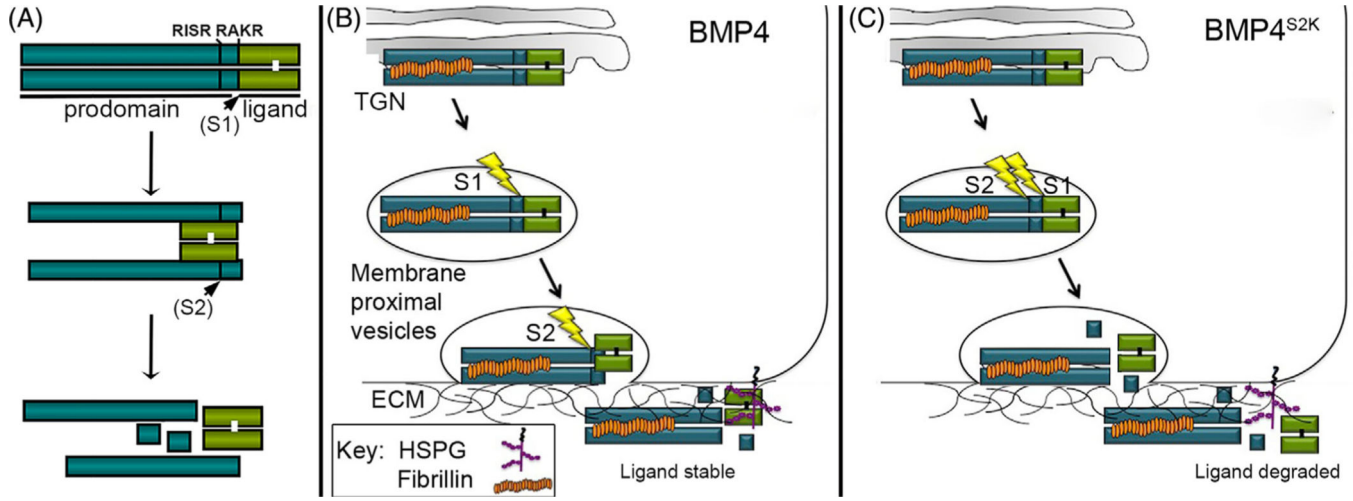

FIGURE 1.

Schematic illustration of proteolytic activation of BMP4. (A) The BMP4 precursor is sequentially cleaved at two sites: initially at a site adjacent to the ligand domain (the S1 site) and subsequently at an upstream site (the S2 site) within the prodomain. The BMP4 ligand forms a transient, non-covalent complex with the prodomain following cleavage at the S1 site, but subsequent cleavage at the S2 site disrupts the complex, freeing the ligand from the prodomain. (B) In our hypothetical model, FBN is bound to the newly synthesized BMP4 precursor, which is then sequentially cleaved at the S1 and S2 sites. We have previously shown that both sites are cleaved in a membrane proximal vesicle and that cleavage is closely coupled to the process of secretion. The transient FBN/prodomain/ligand complex that forms after S1 cleavage ensures that mature BMP4 is deposited in the ECM coincident with S2 cleavage, thereby facilitating association of the ligand with HSPGs or other ECM proteins that are required for ligand stability. (B) We propose that simultaneous cleavage of the S1 and S2 sites of BMP4 in the *Bmp4*^{S2K} mutant mouse leads to premature release of the BMP4 ligand from the FBN/prodomain complex, precluding efficient association with HSPGs or other binding partners that are required for ligand stability.

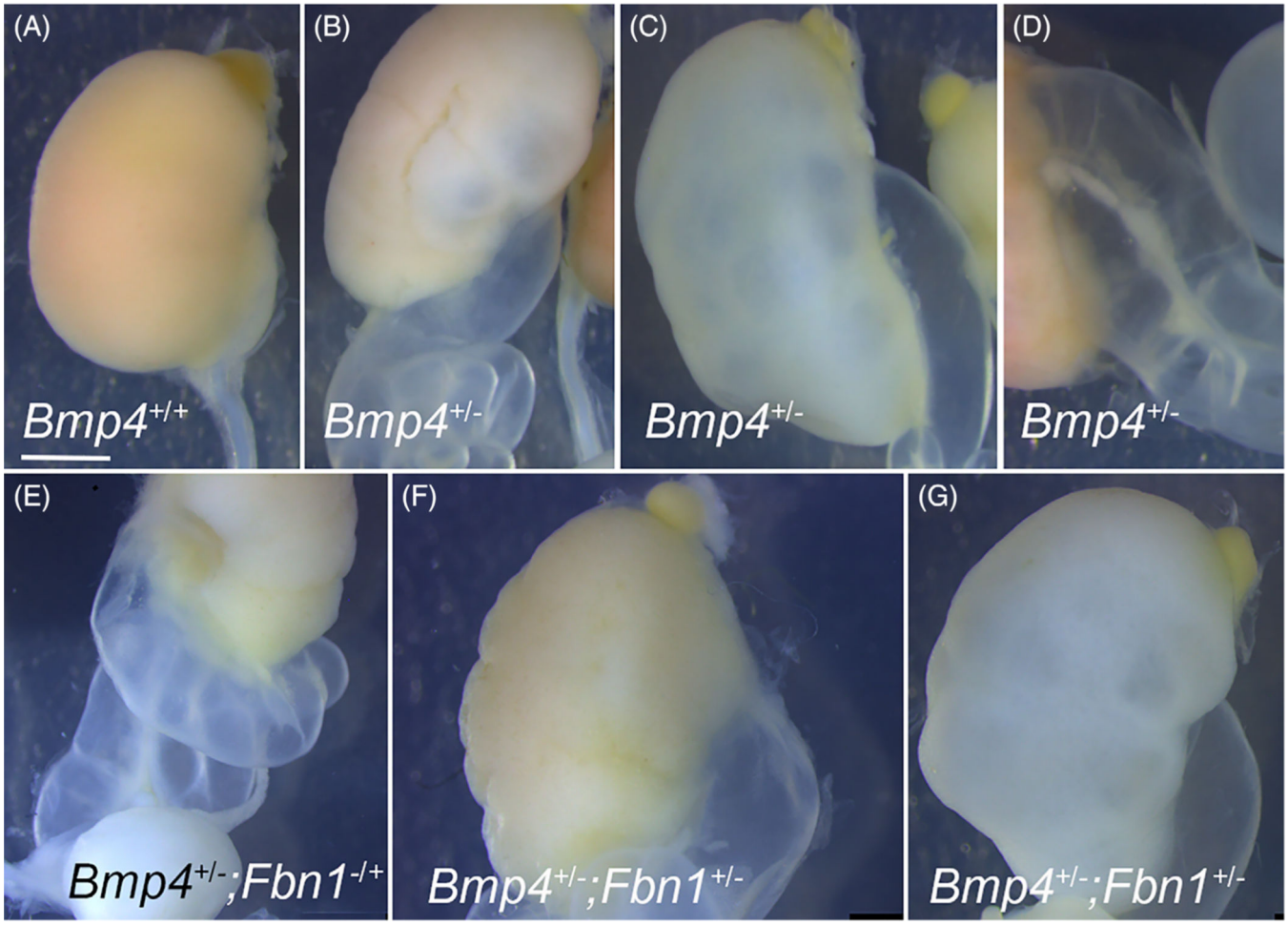

FIGURE 2.

Fbn1$^{+/-}$ and *Bmp4*$^{+/-}$;*Fbn1*$^{+/-}$ mice show kidney defects. (A-G) Photographs of P5 kidneys from wild type mice displaying no defects (A) and kidneys from *Bmp4* $^{+/-}$ (B-D) or *Bmp4* $^{+/-}$;*Fbn1*$^{+/-}$ (E-G) mice displaying hydroureter and hydronephrosis (B, F), hydronephrosis, hydroureter and polycystic kidney (C, G) bifid ureter (D) or hydroureter (E). Scale bar in A is 1 mm and applies to all panels.

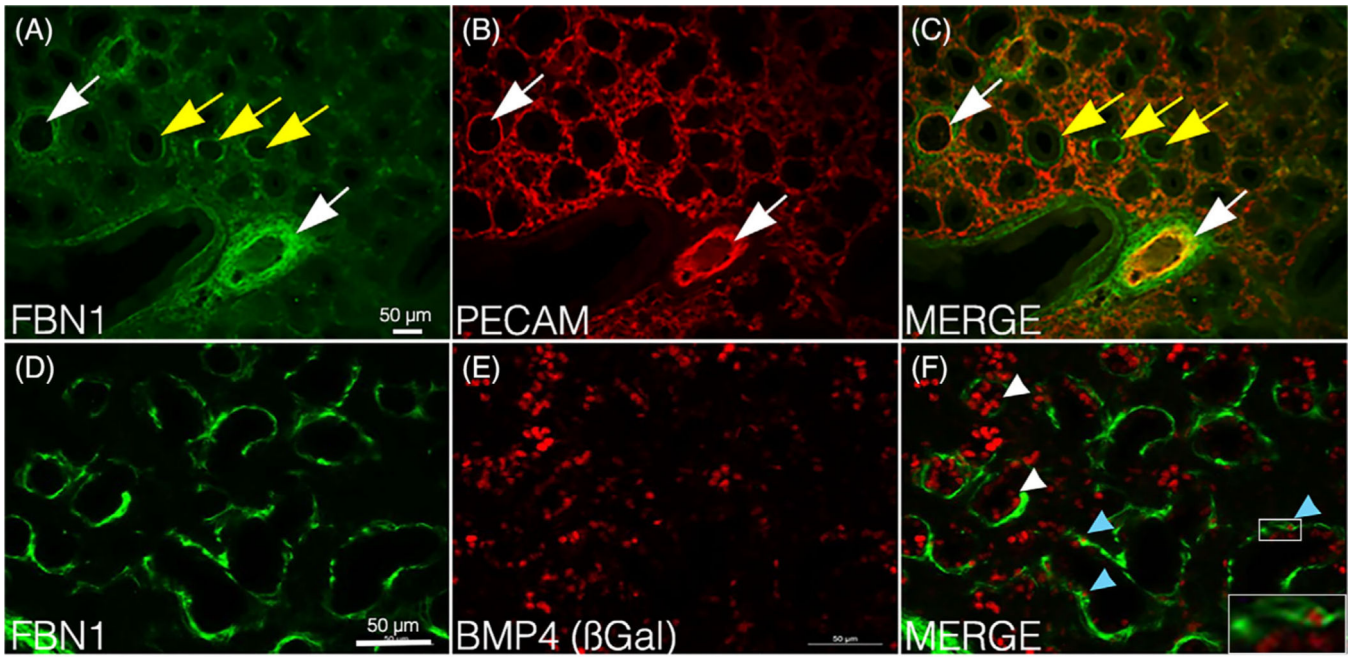

FIGURE 3.

Bmp4 and FBN1 are co-expressed in the lung. (A-F) Cryosections of lungs from E15.5 wild type (A-C) or *Bmp4*$^{+/-}$ (D-F) mice were co-immunostained with antibodies specific for FBN1 and PECAM (A-C) or FBN1 and ß-galactosidase (ßGal) (D-F), which detects *Bmp4* expressing cells. Yellow arrows denote airway epithelial cells, white arrows denote vascular endothelial cells, blue arrowheads denote cells co-expressing *Bmp4* and FBN1, white arrowheads denote *Bmp4* expressing cells adjacent to FBN1 expressing cells. In panel F, an enlarged version of the cell in the small white box is shown in the inset in the bottom right corner to better demonstrate that FBN1 staining is outside of the *Bmp4* expressing, ß-galactosidase positive cell. Results were reproduced a minimum of three times each. Scale bars in panels A and D correspond to 50 μm and apply across each row.

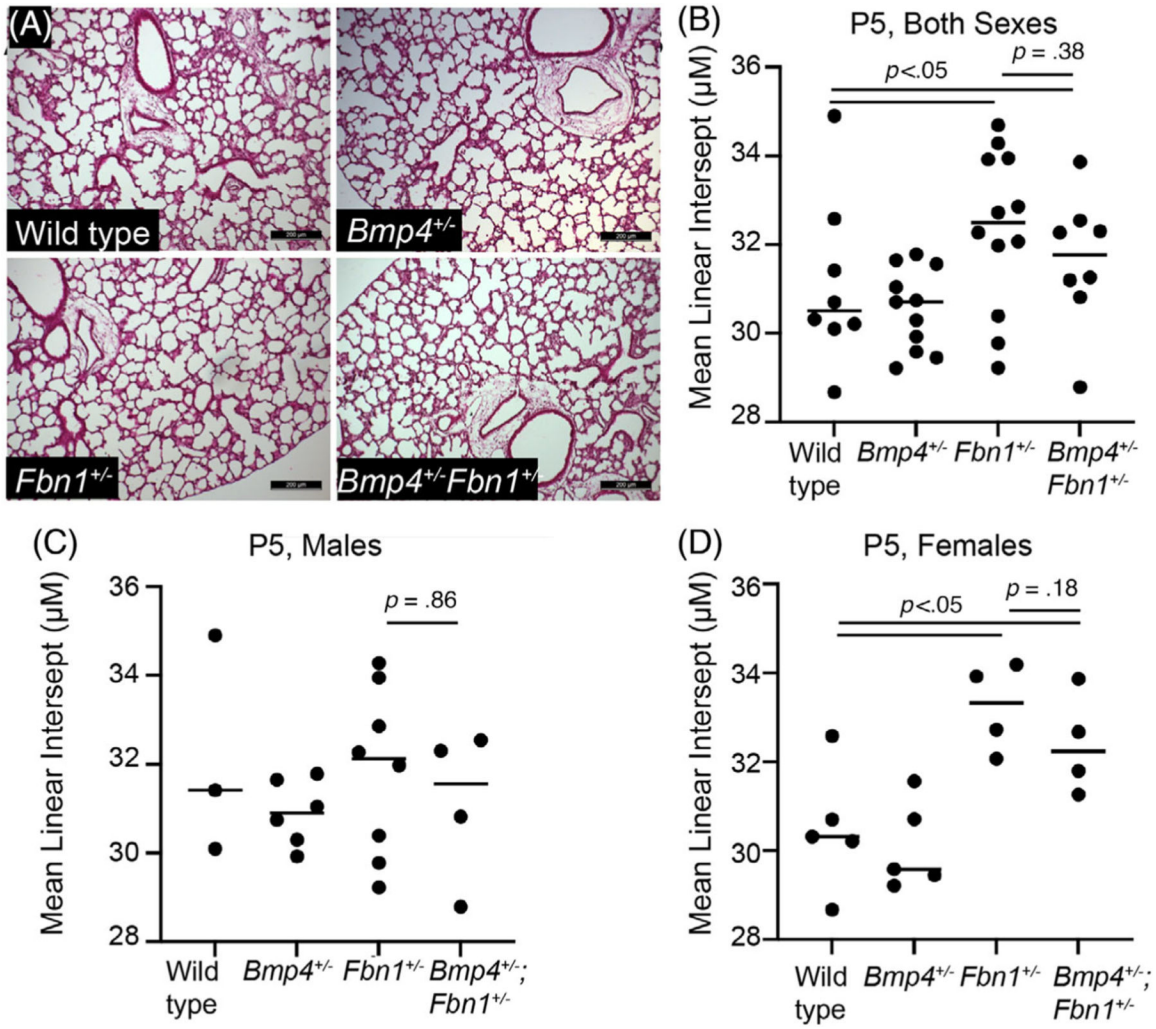

FIGURE 4.

Fbn1$^{+/-}$ and *Bmp4*$^{+/-}$; *Fbn1*$^{+/-}$ female mice show enlarged airspaces in the lungs. (A) Representative histological sections of P5 lungs from female wild type, *Bmp4*$^{+/-}$, *Fbn1*$^{+/-}$ *and Bmp4*$^{+/-}$; *Fbn1*$^{+/-}$ littermates. Scale bars are 200 μm. (B-D) The mean linear intercept, a measure of distal airspace enlargement, was quantified (mean ± SD) at P5 in littermates of both sexes together (B), or in males (C), or females (D) separately.

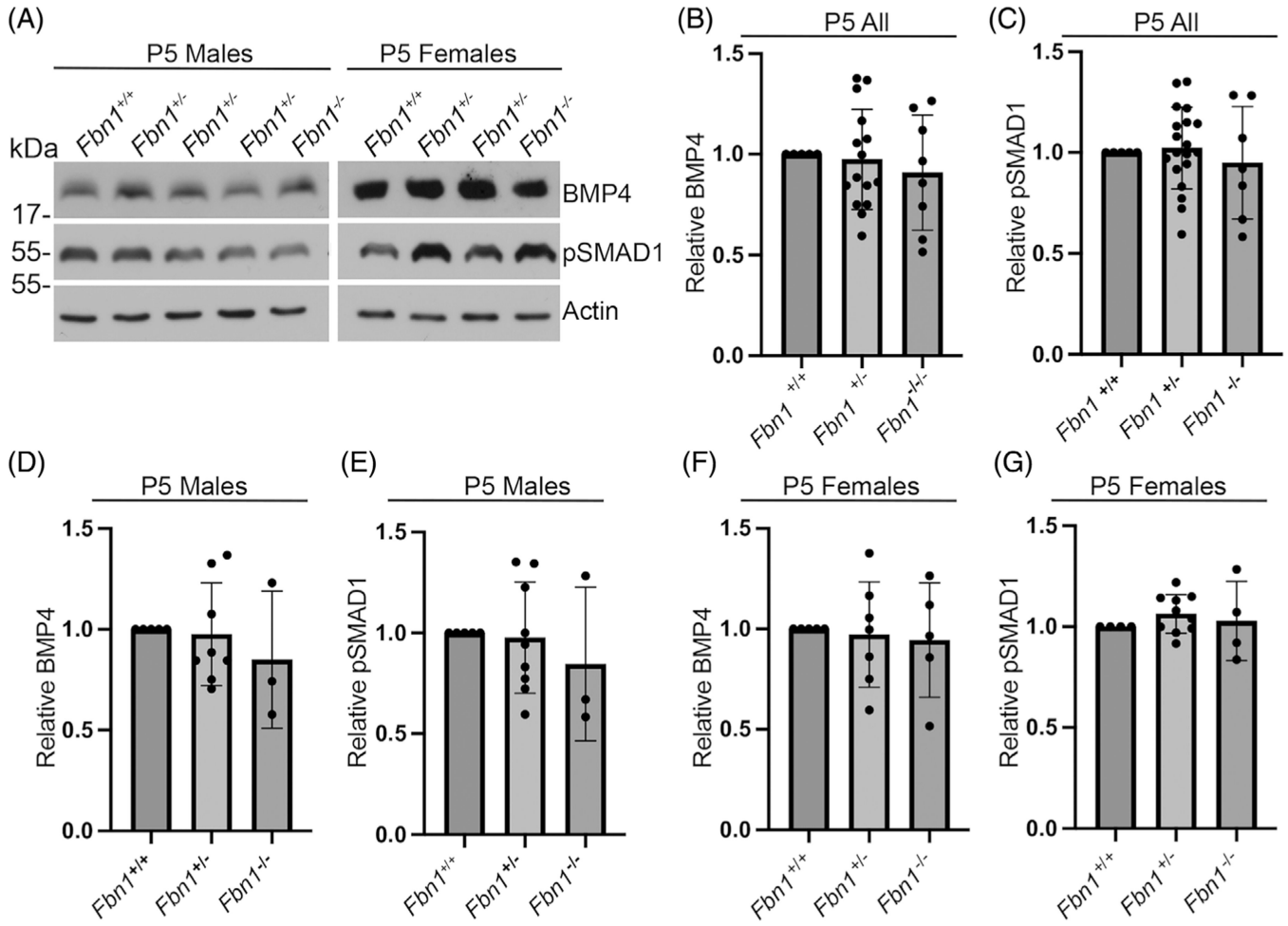

FIGURE 5.

Removal of one or both alleles of *Fbn1* does not alter steady state levels of BMP4 ligand or total BMP activity in P5 lungs. (A) Representative immunoblots of BMP4 ligand and pSMAD1 levels in lungs isolated from P5 male or female littermates. (B-G) BMP4 ligand levels (B, D, F) or pSMAD1 levels (C, E, G) were quantified (mean ± SD) in littermates of both sexes (B-C), males (D-E), or females (F-G).

TABLE 1A

Progeny from *Bmp4*$^{+/-}$ and *Fbn*$^{+/-}$ intercrosses at P21.

Sex	Wildtype	*Fbn1* $^{+/-}$	*Bmp4* $^{+/-}$	*Fbn1* $^{+/-}$ *;Bmp4* $^{+/-}$	*n*	*P-value*
Both	66 (38%)	50 (29%)	32 (18%)	26 (15%)	174	.0005
Male	27 (31%)	26 (30%)	18 (21%)	15 (18%)	86	.1805
Female	37 (42%)	25 (28%)	13 (15%)	13 (15%)	88	.0005

Note: Data are presented as number (percent). *P*-value calculated by chi-square analysis.

Author Manuscript

Author Manuscript

Author Manuscript

TABLE 1B

Progeny from *Bmp4*$^{+/-}$ and *Fbn*$^{+/-}$ intercrosses at P8.

Sex	Wildtype	*Fbn1* $^{+/-}$	*Bmp4* $^{+/-}$	*Fbn1* $^{+/-}$ *;Bmp4* $^{+/-}$	n	*P-value*
Both	29 (29%)	35 (35%)	17 (17%)	19 (19%)	100	.0345
Male	17 (30%)	15 (26%)	11 (19%)	14 (25%)	57	.7253
Female	12 (28%)	20 (47%)	6 (14%)	5 (11%)	43	.0041

Note: Data are presented as number (percent). *P*-value calculated by chi-square analysis.

TABLE 1C

Progeny from *Bmp4*$^{+/-}$ and *Fbn*$^{+/-}$ intercrosses at P6.

Sex	Wildtype	*Fbn1* $^{+/-}$	*Bmp4* $^{+/-}$	*Fbn1* $^{+/-}$ *;Bmp4* $^{+/-}$	n	*P-value*
Both	48 (28%)	53 (31%)	32 (19%)	37 (22%)	170	.0853
Male	23 (25%)	30 (33%)	20 (22%)	18 (20%)	91	.3034
Female	25 (32%)	23 (29%)	12 (15%)	19 (24%)	79	.1718

Note: Data are presented as number (percent). *P*-value calculated by chi-square analysis.